Electronic Supplementary Material (ESI) for Journal of Materials Chemistry B.

Supporting Information

A Combination of Graphene Quantum Dots-Cationic Red Dye Donor-Acceptor Pair and Cucurbit[7]uril as Supramolecular Sensor for Ultrasensitive Detection of Cancer Biomarkers Spermine and Spermidine

Akhil A. Bhosle,[a] Mainak Banerjee,[a] Sharanabasava D. Hiremath,[a] Dilawar S. Sisodiya,[a] Viraj G. Naik,[a] Nilotpal Barooah,[b] Achikanath C. Bhasikuttan,[b,c] Anjan Chattopadhyay,[a] Amrita Chatterjee*[a]*

[a]Department of Chemistry, BITS Pilani, K. K. Birla Goa Campus, NH 17B Bypass Road, Zuarinagar, Goa 403726, INDIA
[b]Radiation & Photochemistry Division, Bhabha Atomic Research Centre, Trombay, Mumbai, INDIA
[c]Homi Bhabha National Institute, Anushaktinagar, Mumbai, INDIA

Corresponding Authors
*E-mail: mainak@goa.bits-pilani.ac.in. Phone: +91-832-2580-347. Fax: +91-832-255-7031 (M.B.).
*E-mail: amrita@goa.bits-pilani.ac.in. Phone: +91-832-2580-320. Fax: +91-832-255-7031 (A.C.).

Table of Contents

Experimental Procedure

Synthesis of hydroxy graphene quantum dots (HO-GQDs):[1] Pyrene (0.2 g) was refluxed in conc. HNO_3 (16 mL) at 95 °C for 12 h. The mixture was then cooled to room temperature and diluted with 100 mL of deionized water, and filtered to obtain yellow 1,3,6- trinitropyrene (0.26 g). Next, the yellow product was dispersed in a 60 mL of 0.2 M NaOH solution by ultrasonication for 2 h. Then the suspension was transferred to a Teflon autoclave container and heated at 200 °C for 10 h. The product containing water-soluble GQDs was filtered through a 0.22 μm microporous membrane to remove insoluble carbon product after cooling to room temperature and further dialyzed in a dialysis bag (retained molecular weight: 10,000 Da) for 2 days to remove sodium salt and unfused small molecules. The purified black OH-GQDs were dried at 80 °C and characterized using standard techniques.

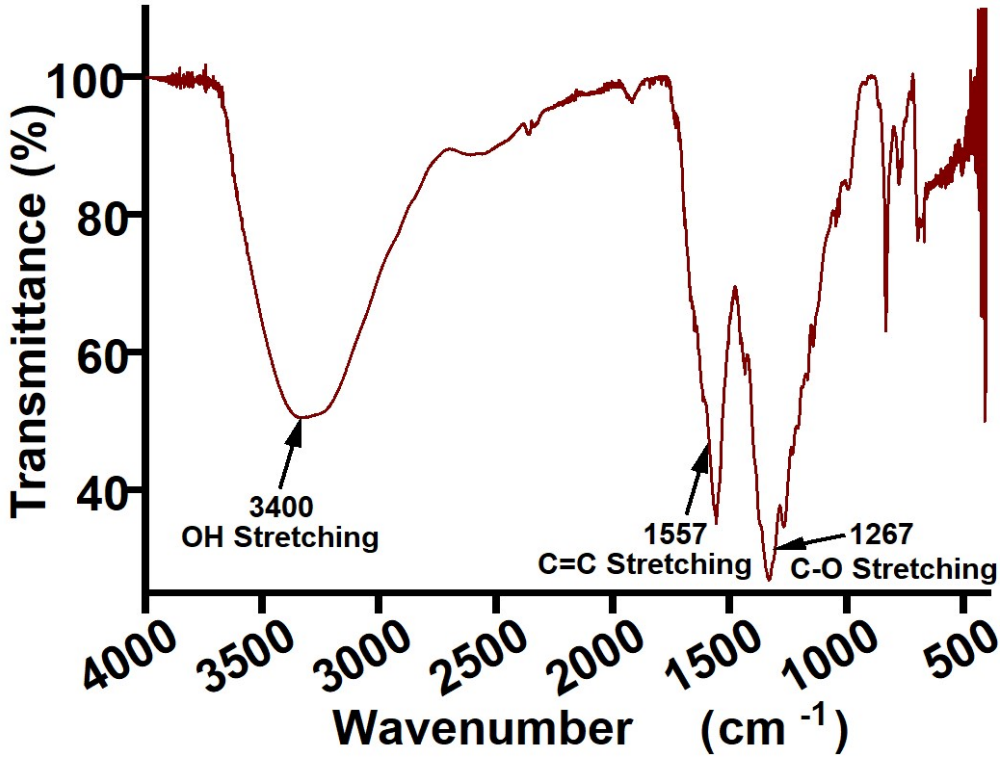

Figure S1. IR spectra confirm the presence of hydroxyl groups in the HO-GQDs.

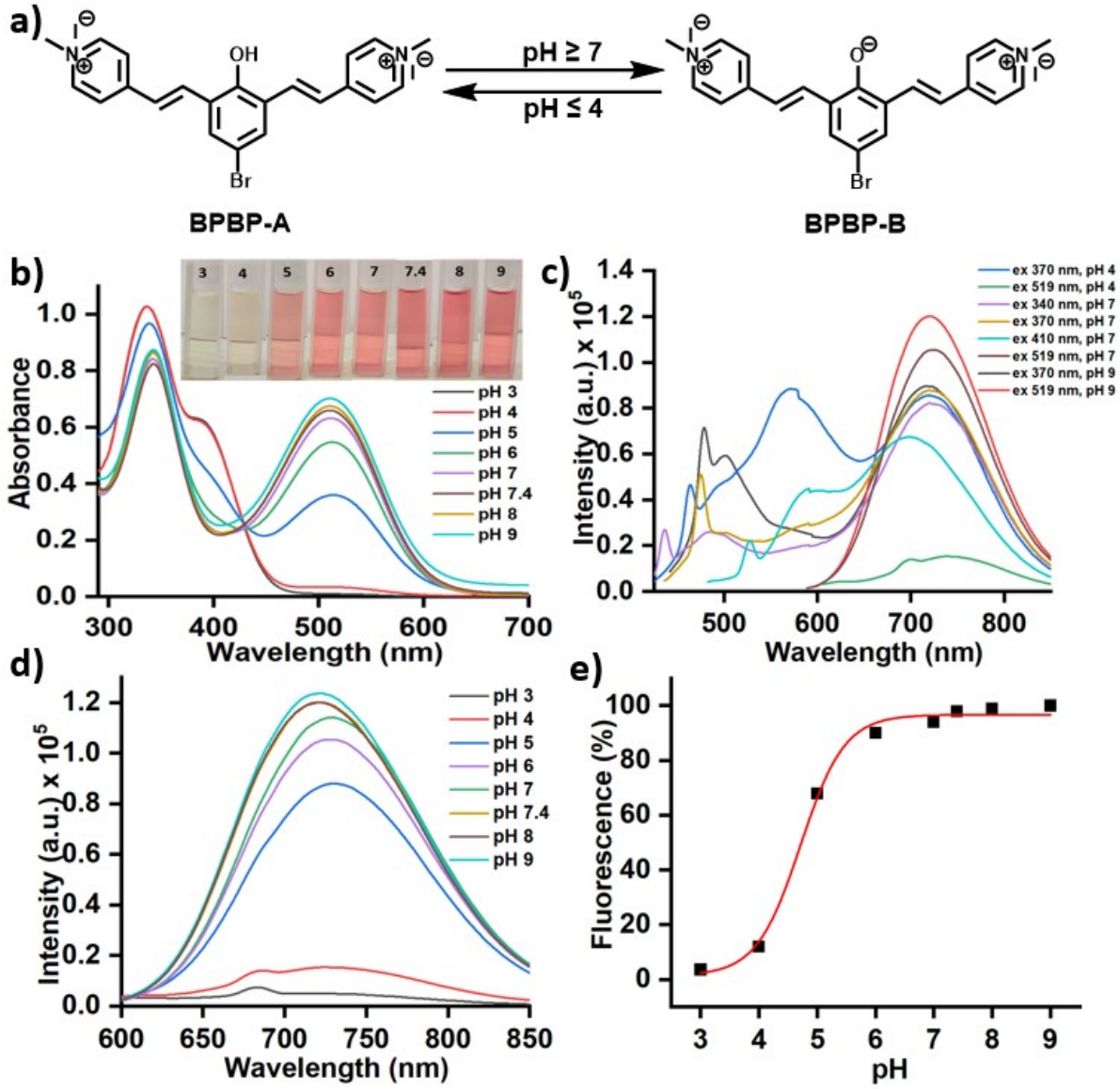

Figure S2. (a) Protonated and deprotonated forms of **BPBP**; (b) Response of **BPBP** at different pH in UV-vis; (c) fluorimetric responses of **BPBP** at different excitation wavelengths and pH; (d) Response of **BPBP** at different pH in fluorimetric studies; (e) Plot of % fluorescence v/s pH for determination of pK_a.

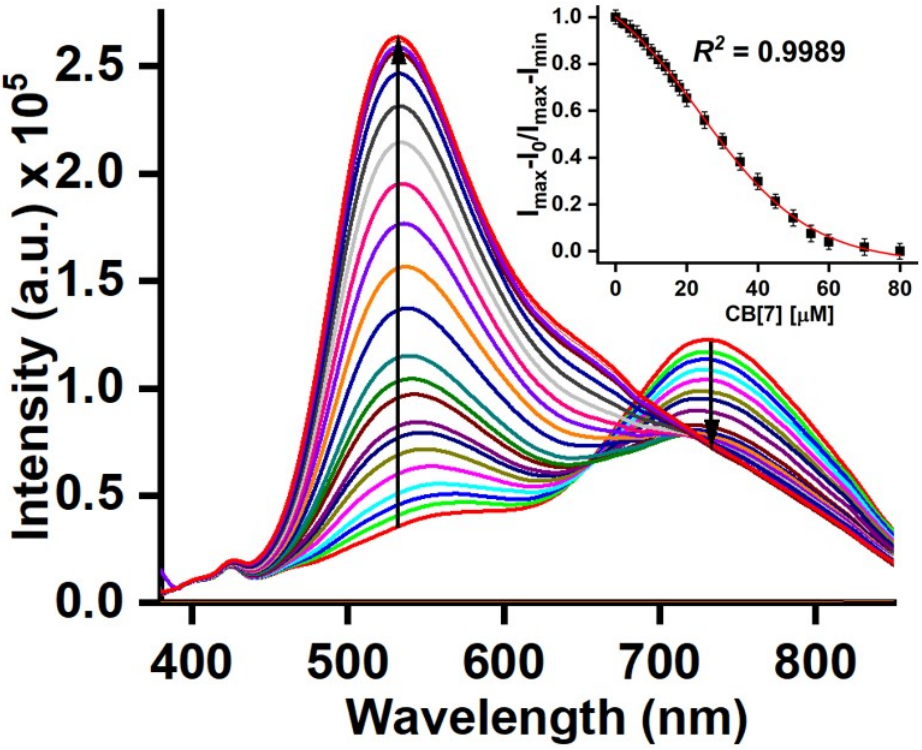

Figure S3. The fluorimetric responses of GQDs (5 μL, 1 mg/mL) + **BPBP** (30 μM) upon the addition of CB[7] (0-100 μM) showed an increase in intensity at 535 nm and a simultaneous ratiometric decrease in intensity at 730 nm [GQDs: λ_{ab} 370 nm, λ_{em} 545 nm; **BPBP**: λ_{ab} 519 nm, λ_{em} 730 nm].

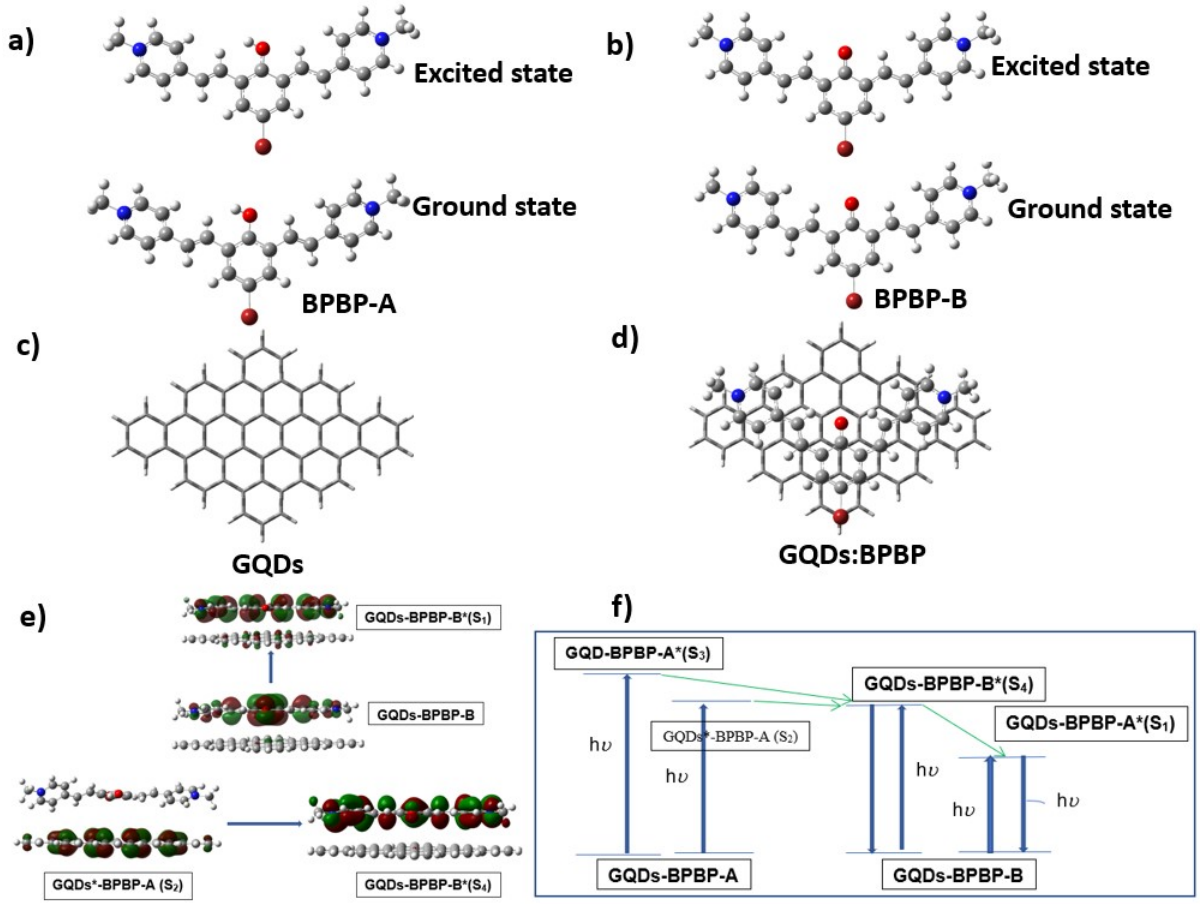

Figure S4. Optimized structures of (a) ground state and excited state **BPBP-A**; (b) ground state and excited state **BPBP-B**; (c) GQDs; (d) GQDs:BPBP complex top view; (e) HOMO →LUMO excitation of GQDs-BPBP-B which dominates the 526 nm peak (S_0-S_1) and LUMO+2 orbitals GQDs-BPBP-A and GQDs-BPBP-B involved in the quenching of GQDs fluorescence and (f) A schematic representation of the fate of photo-excitations of GQDs-BPBP-A and GQDs-BPBP-B.

Table S1. Predicted absorption peak positions (with oscillator strength of the transition and dominating excitations in %) and emission peak positions of **BPBP** forms in water at TDDFT level.

	Predicted Absorption peak positions (at TDDFT) λ_{abs} **(nm)**	Oscillator strength of the transition	Contributed by excitations (with major contributions in %)
BPBP-A	361 (λ_{em} = 464 nm)	1.6992	H→L (73%), H-1→L (13%)
BPBP-B	550 400 (λ_{em} = 708 nm)	1.3620 0.1940	H→L (89%) H→L+1 (67%), H-1→L (26%)
BPBP-A-CB[7] (1:1)	416 343	0.8893 0.6318	H→L (83%) H-1→L (75%)
BPBP-A-CB[7] (2:1)	399 351	0.898 0.1029	H→L (65%), H→L+1 (11%) H→L+1 (55%), H-1→L (22%)
GQDs	376	0.3222	
GQDs-BPBP-A	376 350	0.2786 0.4137	H→L+2 (76%), H-1→L+3 (14%) H-3→L (55%), H-4→L (16%), H-5→L+1 (10%)
GQDs-BPBP-B	526 378 365	0.6896 0.1959 0.1019	H→L (84.5%) H→L+2 (66%), H-4→L(15%) H→L+1 (72%)

Table S2. Some important orbitals of GQDs-BPBP-A and GQDs-BPBP-B contributing to the mentioned absorption peaks

GQDs-BPBP-A	
H-4	L
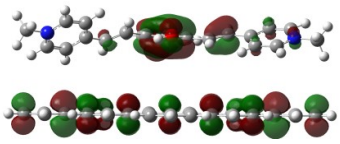	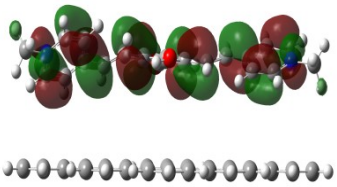
H-3	L+1
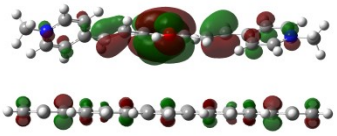	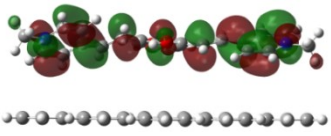
H-1	L+2
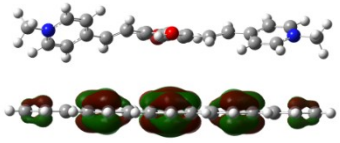	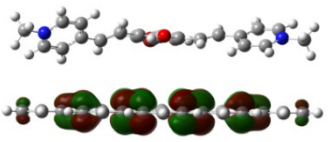

H	L+3
GQDS-BPBP-B	
H	L
	L+1
	L+2

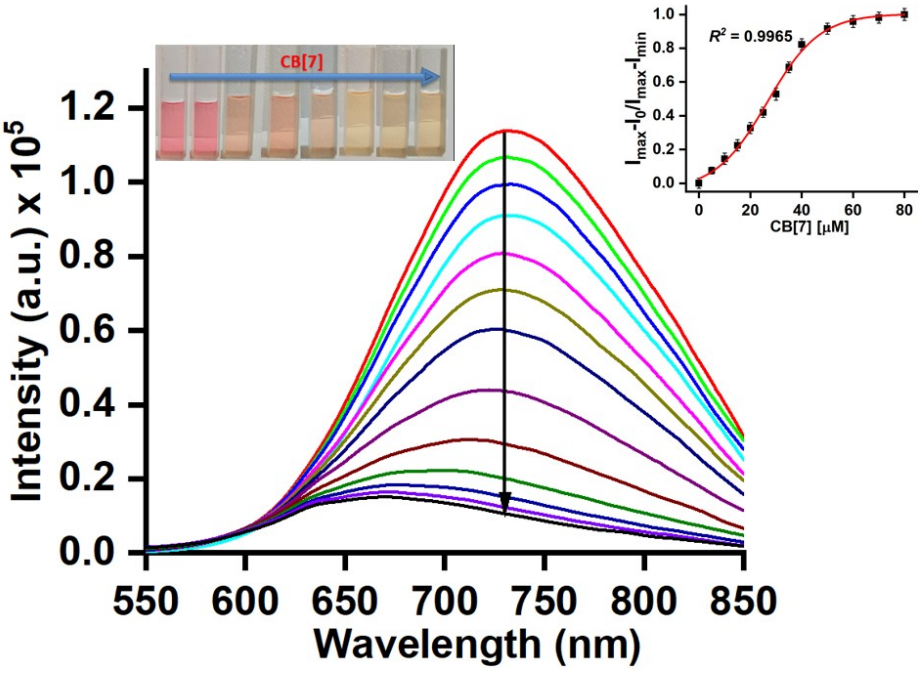

Figure S5. Fluorescence response of **BPBP** (30 μM) upon addition of CB[7] (0-80 μM) shows a decrease in intensity along with a visual color change from red to yellow [λ_{ex} 519 nm, λ_{em} 730 nm].

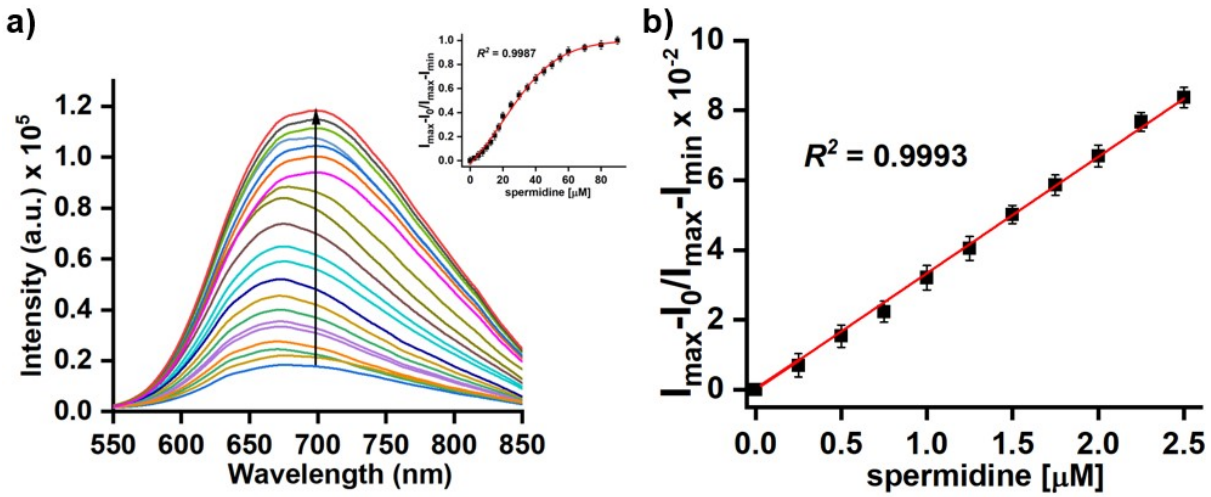

Figure S6. (a) Fluorescence response of **BPBP** (30 μM) + CB[7] (60 μM) upon addition of spermidine (0-80 μM) [λ_{ex} 519 nm, λ_{em} 730 nm]; (b) Fluorescence response of sensing assembly containing 30 μM **BPBP** at the lower concentration range for spermidine (0−2.5 μM) [λ_{ex} 519 nm, λ_{em} 730 nm].

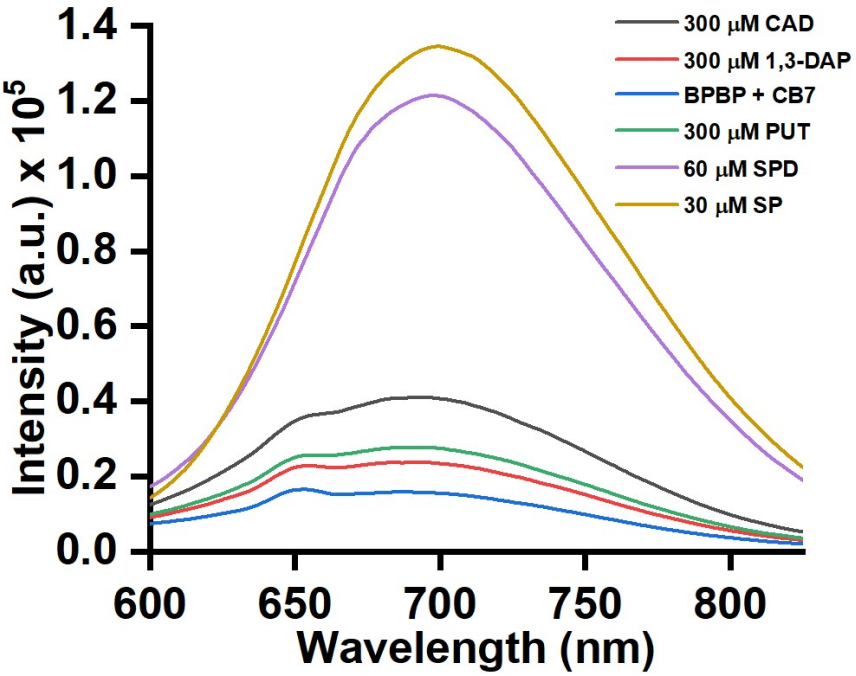

Figure S7. Fluorescence response of the two-component supramolecular assembly against biogenic amines [λ_{ex} 519 nm, λ_{em} 730 nm].

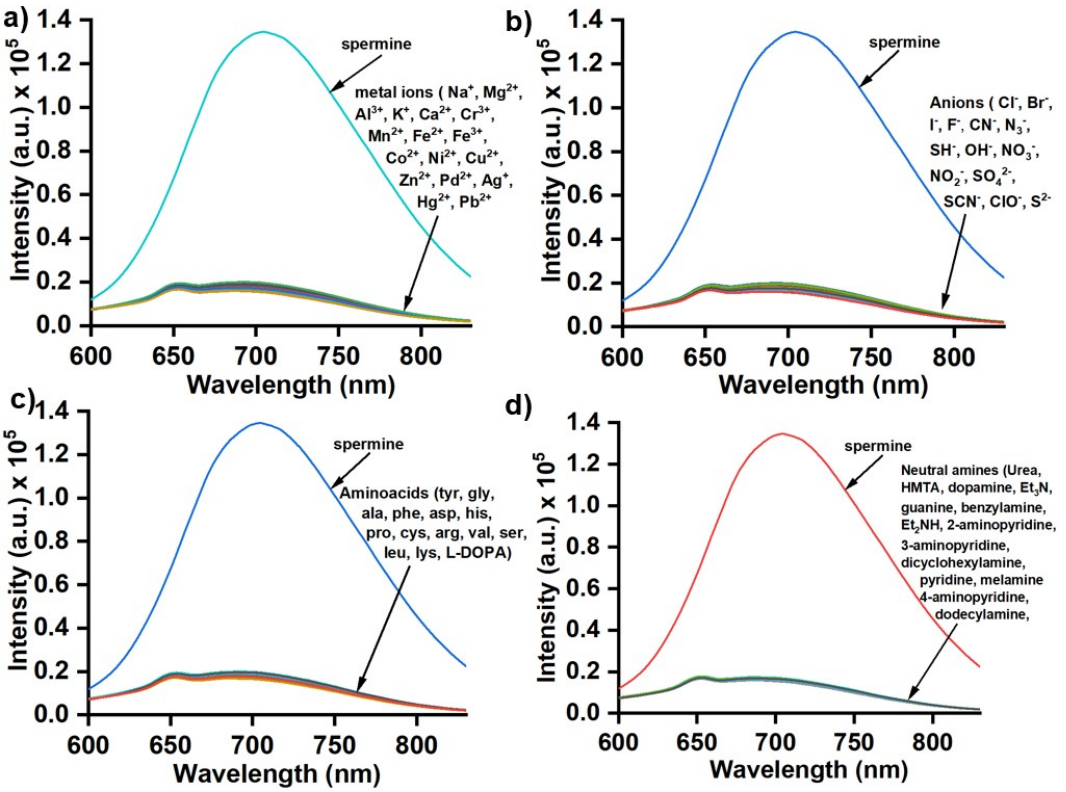

Figure S8. Fluorescence response of the two-component supramolecular assembly against (a) metal ions; (b) anions; (c) amino-acids; (d) neutral molecules [λ_{ex} 519 nm, λ_{em} 730 nm].

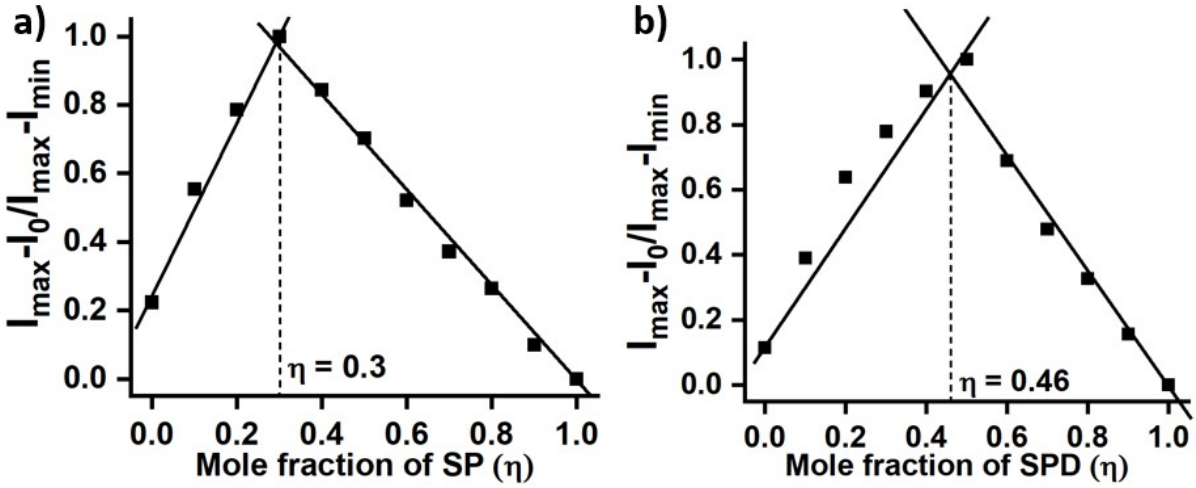

Figure S9. Job's plot for the determination of the stoichiometry of BPBP:CB[7] two-component assembly [**BPBP** (30 μM), CB[7] and SP/SPD concentration varied between 0-30 μM (λ_{ex} 519 nm; λ_{em} 730 nm).

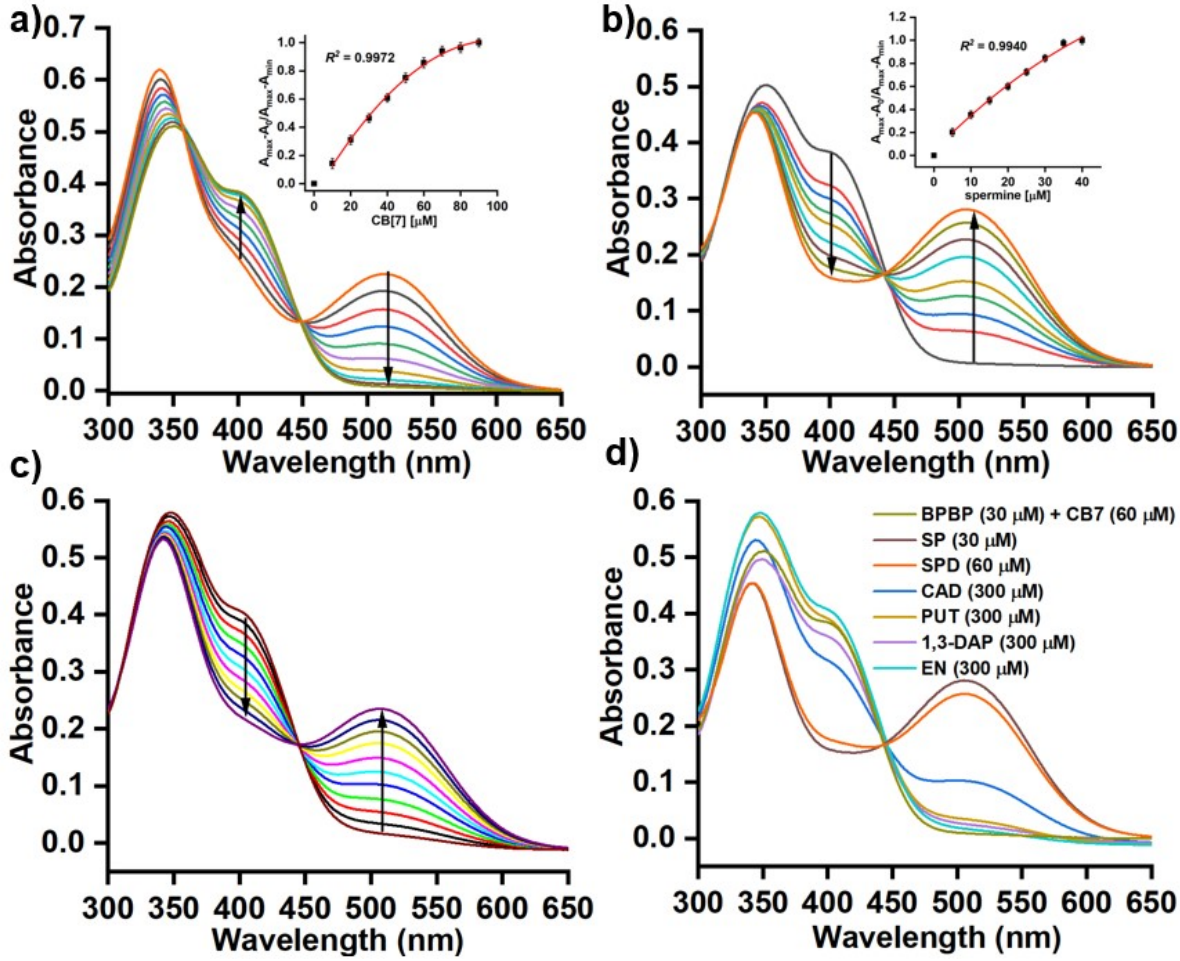

Figure S10. UV-vis spectra of (a) **BPBP** (30 μM) upon addition of CB[7] (0-100 μM); (b) **BPBP** (30 μM) + CB[7] (60 μM) upon addition of spermine (0-40 μM); (c) **BPBP** (30 μM) + CB[7] (60 μM) upon addition of spermidine (0-70 μM) in water; (d) Response of the two-component supramolecular assembly against biogenic amines.

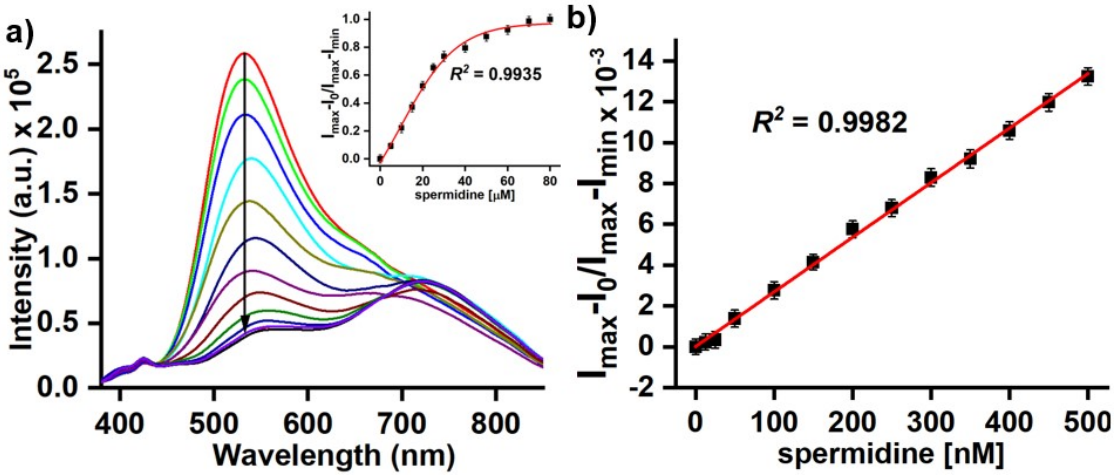

Figure S11. (a) Fluorescence response of GQDs (5 μL, 1 mg/mL) + **BPBP** (30 μM) + CB[7] (60 μM) upon addition of spermidine (0-80 μM); (b) Fluorescence response of sensing assembly containing 30 μM **BPBP** at the lower concentration range for spermidine (0−500 nM) (LOQ = 12.5 nM, LOD = 0.9 ppb) (GQDs λ_{ex} 370 nm, λ_{em} 545 nm; **BPBP** λ_{em} 730 nm).

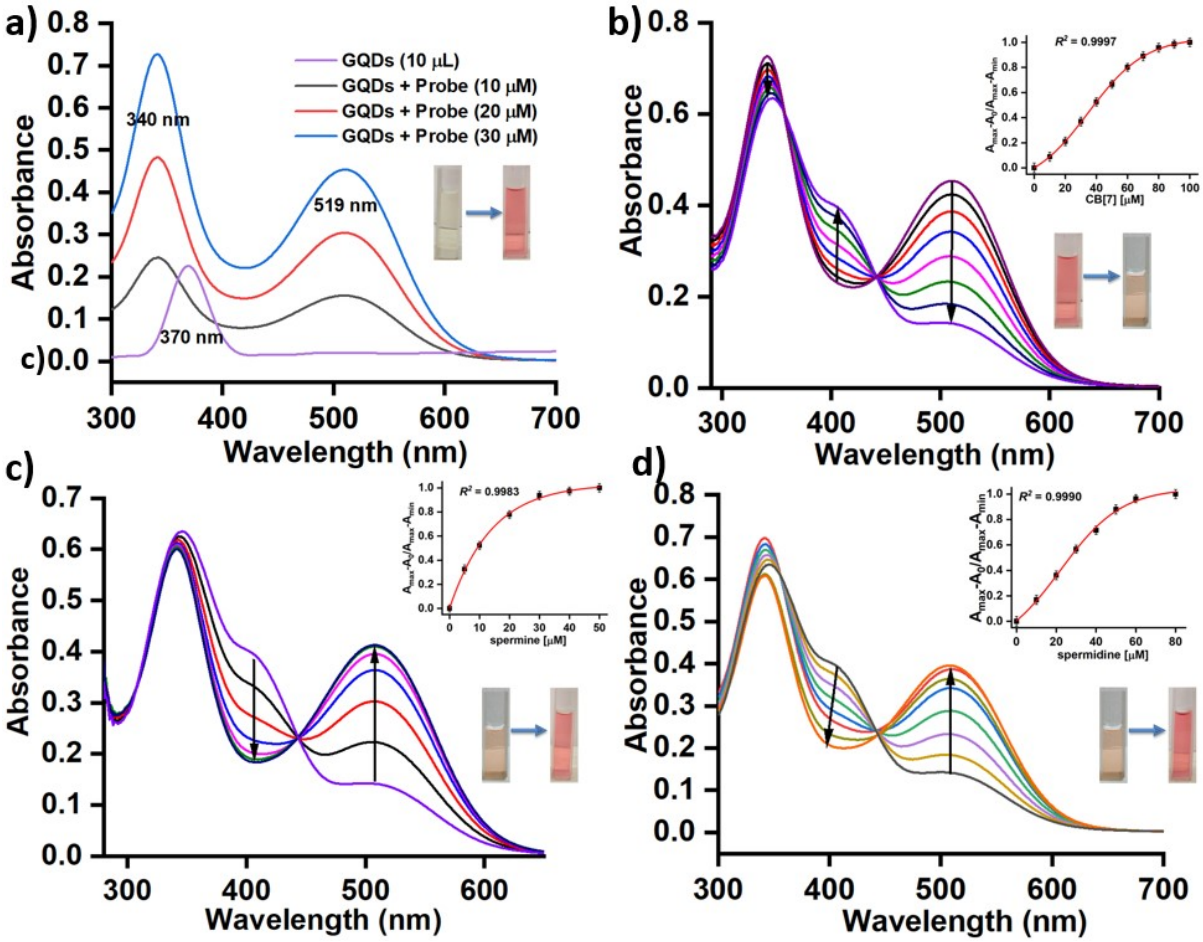

Figure S12. UV-vis spectra of GQDs upon addition of (a) **BPBP** (0-30 μM); (b) **BPBP** (30 μM) + CB[7] (0-100 μM); (c) **BPBP** (30 μM) + CB[7] (60 μM) + spermine (0-40 μM); (d) **BPBP** (30 μM) + CB[7] (60 μM) + spermidine (0-80 μM) in water.

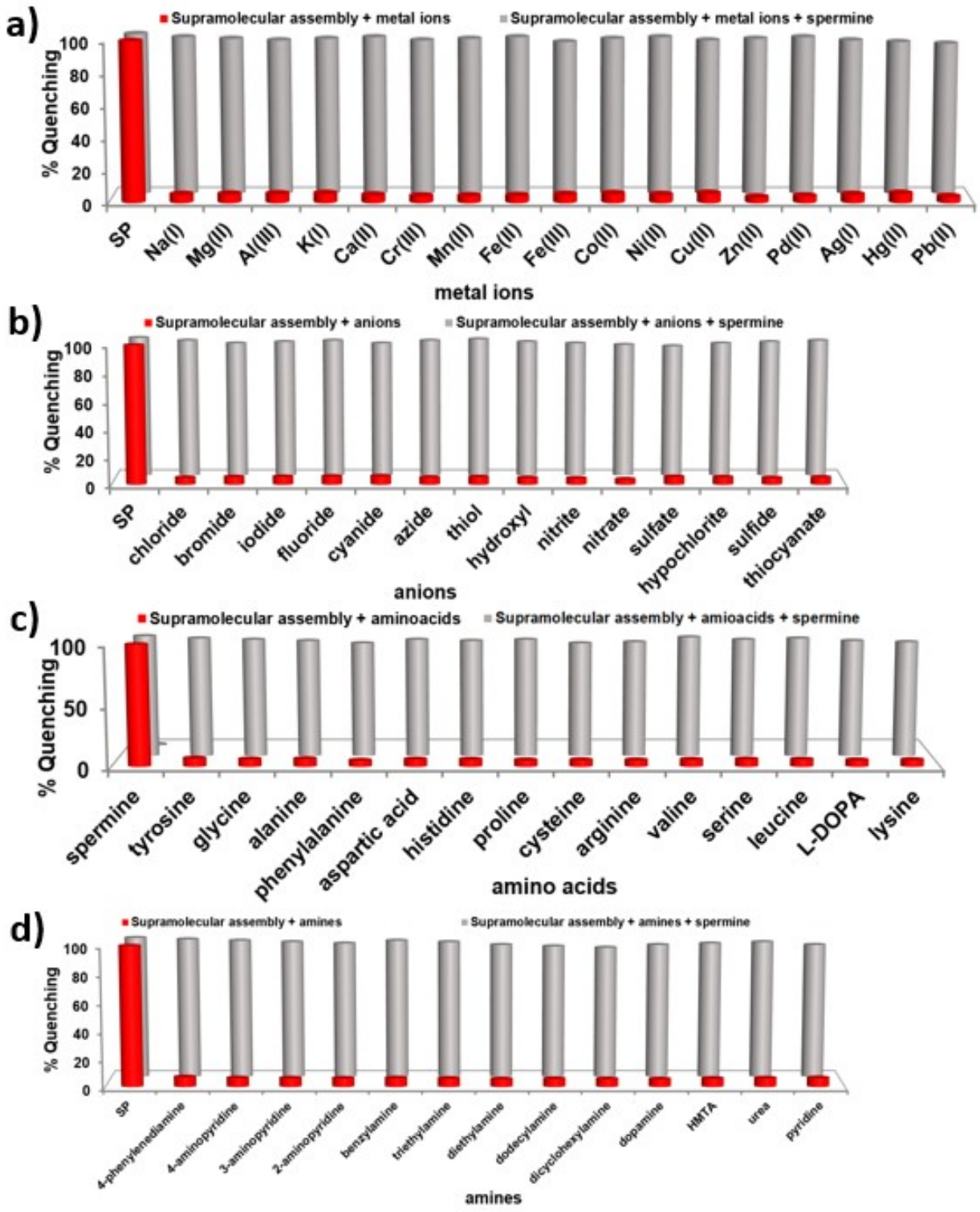

Figure S13. Percentage fluorescence quenching of the supramolecular assembly (at λ_{em} 535 nm) with (a) metal ions; (b) anions; (c) amino acids; (d) neutral molecules [red bars]; and corresponding competitive study in the presence of spermine (30 μM) [grey bars].

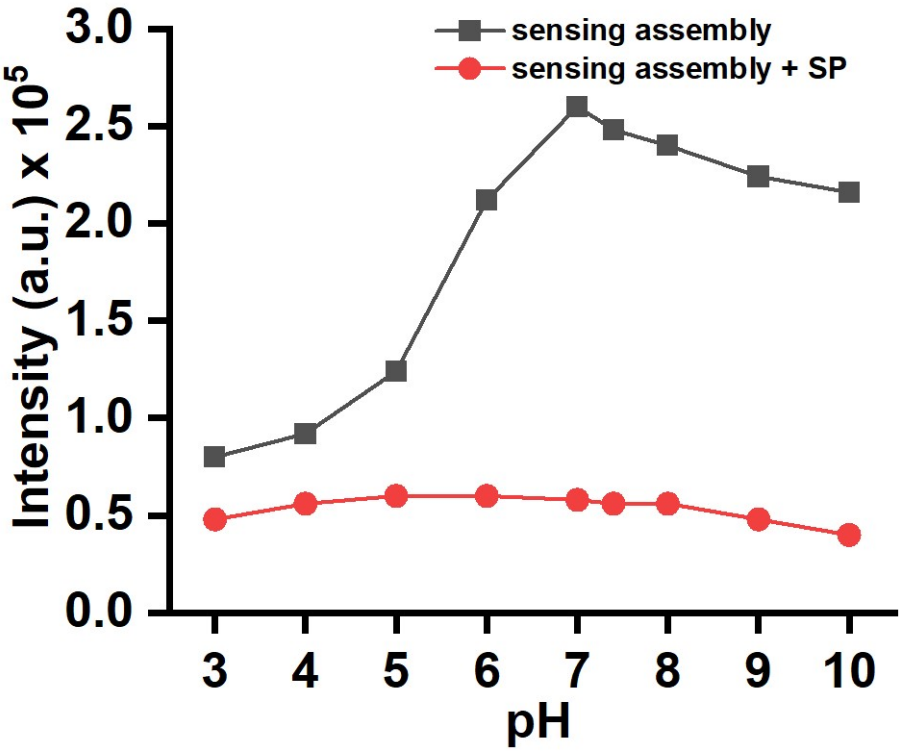

Figure S14. Effect of pH on the relative emission intensities of GQDs:BPBP:CB[7] supramolecular sensing assembly containing 30 μM **BPBP**; and sensing assembly upon addition of spermine (30 μM) [λ_{ex} 370 nm, λ_{em} 535 nm].

Table S3. Life-time decay trace of **BPBP**, **BPBP** + CB[7], and **BPBP** + CB[7] upon addition of spermine.

System	τ_1/ns (%)	τ_2/ns (%)	τ_3/ns (%)	χ^2	τ_{av}/ns
BPBP in water (λ_{ex} 511 nm, λ_{em} 730 nm)	0.06 (82)	0.25 (13)	1.03(5)	1.20	0.133
BPBP + CB[7] in water (λ_{ex} 511 nm, λ_{em} 730 nm)	0.14 (38)	0.85 (35)	2.63 (27)	1.24	1.061
BPBP + CB[7] + SP in water (λ_{ex} 511 nm, λ_{em} 730 nm)	0.07 (76)	0.24 (18)	1.01 (6)	1.30	0.157

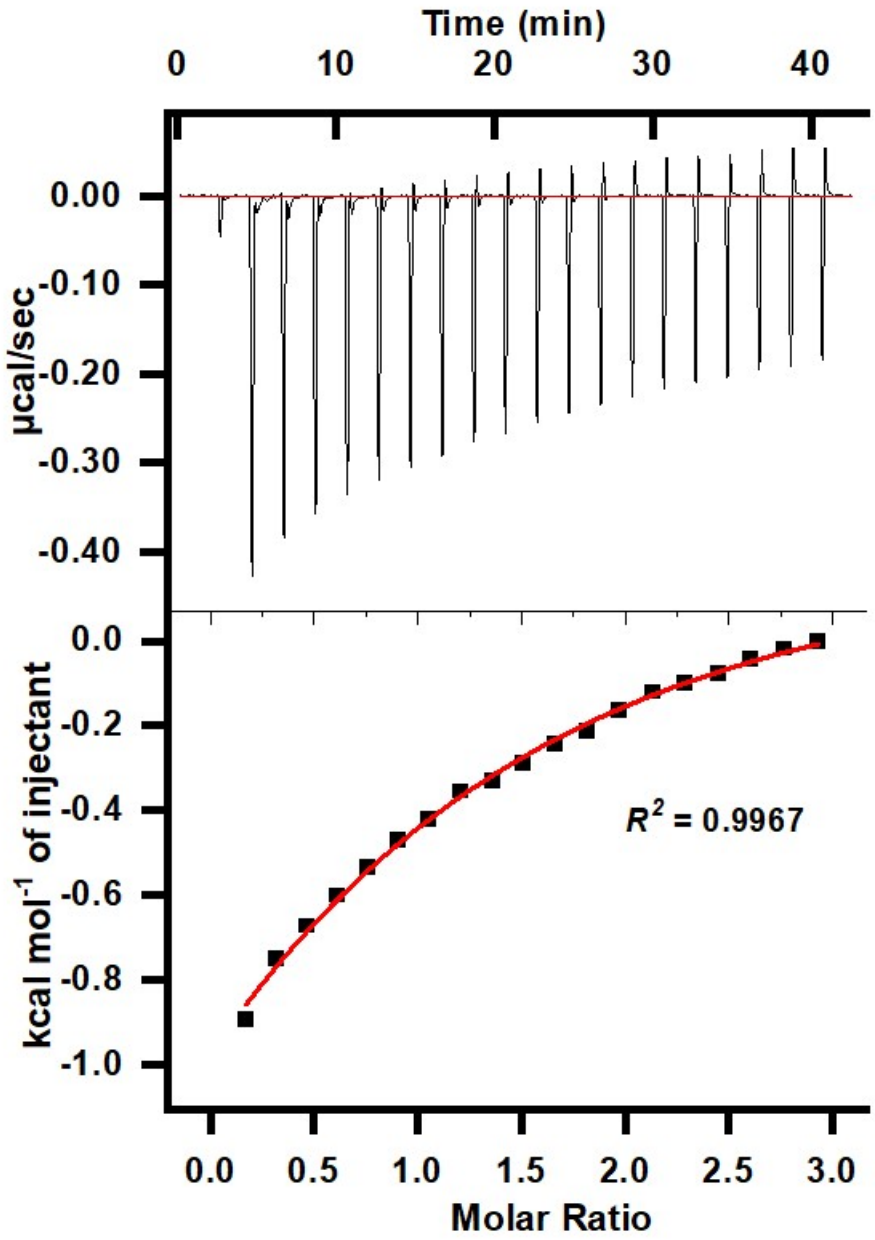

Figure S15. Isothermal calorimetric titration for host-guest complexation of **BPBP** and CB[7]. (A) Raw data for the titration of CB[7] with **BPBP** in the Tris.HCl buffer pH 7.4 at 25 °C, showing the calorimetric response as successive injections of the CB[7] are added to the sample cell. (B) The integrated heat profile of the calorimetric titration is shown in panel A. The solid line represents the best nonlinear least-squares fit in a 1:2 (BPBP:CB[7]) one-site binding model.

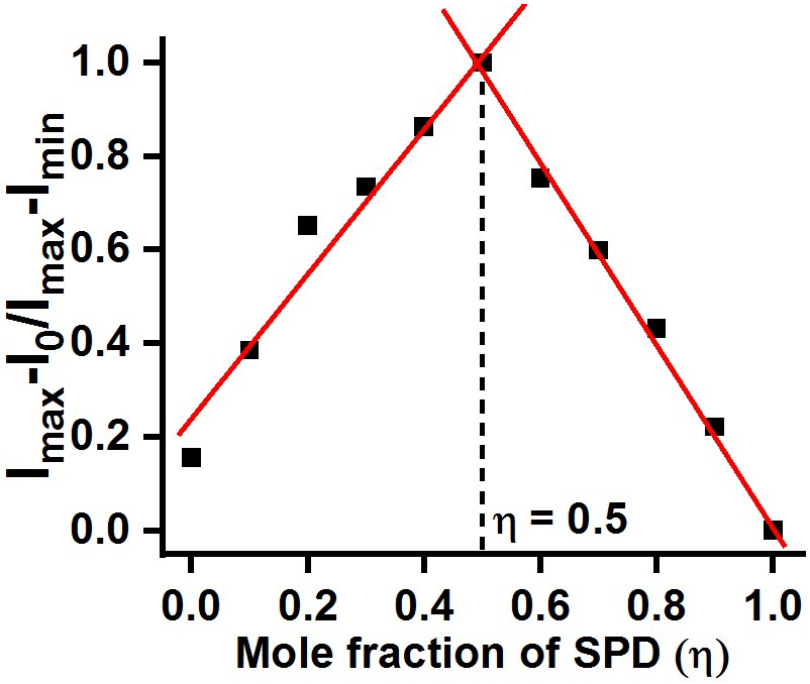

Figure S16. Job's plot for the determination of the stoichiometry of GQDs:BPBP:CB[7] three-component assembly [**BPBP** (30 μM), GQDs 5 μL, 1 mg/mL, CB[7] and SPD concentration varied between 0-30 μM (λ_{ex} 370 nm; λ_{em} 535 nm).

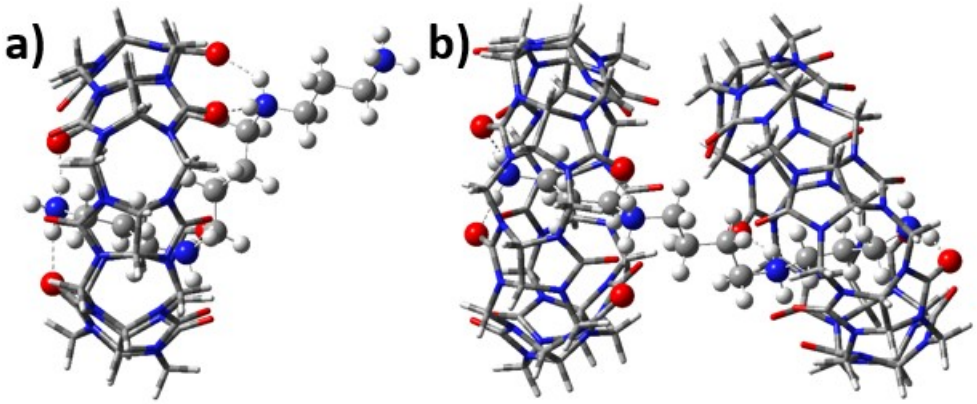

Figure S17. DFT optimized structures of 1:1 and 2:1 CB[7]:SP complex.

Table S4. Life-time decay trace of **BPBP**, GQDs:BPBP conjugate, GQDs:BPBPCB[7] assembly with different concentrations of spermine and spermidine.

System	τ_1/ns (%)	τ_2/ns (%)	τ_3/ns (%)	χ^2	τ_{av}/ns
BPBP in water (λ_{ex} 511 nm, λ_{em} 730 nm)	0.06 (82)	0.25 (13)	1.03 (5)	1.20	0.133
GQDs (λ_{ex} 374 nm, λ_{em} 535 nm)	0.25 (27)	1.85 (34)	5.15 (39)	1.19	2.71
GQDs-BPBP (λ_{ex} 374 nm, λ_{em} 535 nm)	0.22 (18)	0.85 (33)	2.81 (49)	1.06	1.69
GQDs-BPBP (λ_{ex} 374 nm, λ_{em} 730 nm)	0.05(63)	0.36(20)	3.24 (17)	1.07	0.654
GQDs-BPBP-CB[7] (λ_{ex} 374 nm, λ_{em} 535 nm)	0.07 (50)	0.48 (17)	3.76 (33)	1.06	1.36
GQDs-BPBP-CB[7]-SP (λ_{ex} 374 nm, λ_{em} 535 nm)	0.20 (21)	1.32 (56)	4.46 (23)	1.2	1.81

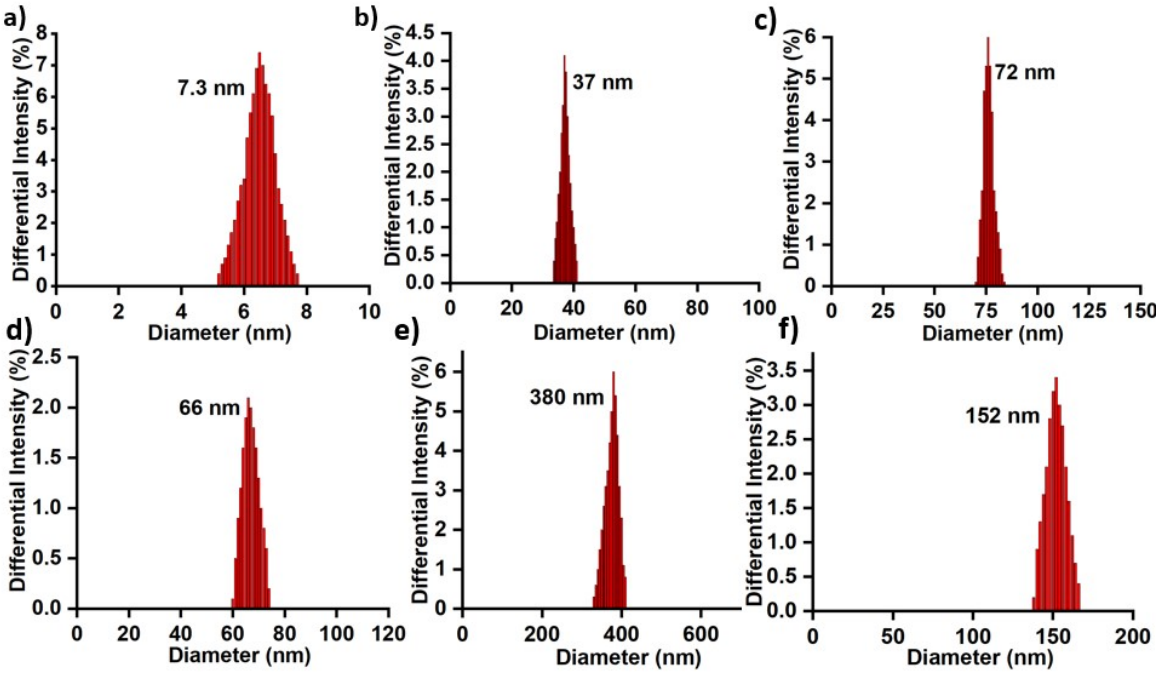

Figure S18. Particle size analysis of (a) GQDs; (b) **BPBP**; (c) CB[7]; (d) GQDs:BPBP conjugate; (e) GQDs:BPBP:CB[7] assembly; (f) after addition of spermine in the aqueous solution of the assembly.

Table S5. Zeta potential data for the individual components, binary conjugate, three-component sensing assembly, and sensing assembly upon the addition of spermine.

Sample	**BPBP**	**GQDs**	**CB[7]**	**Spermine**	**GQDs + BPBP**	**GQDs + BPBP + CB[7]**	**GQDs + BPBP + CB[7] + spermine**
Zeta potential (ζ)	+5.07 mV	−7.35 mV	−12.03 mV	+ 0.45 mV	−1.54 mV	−15.10 mV	−7.64 mV

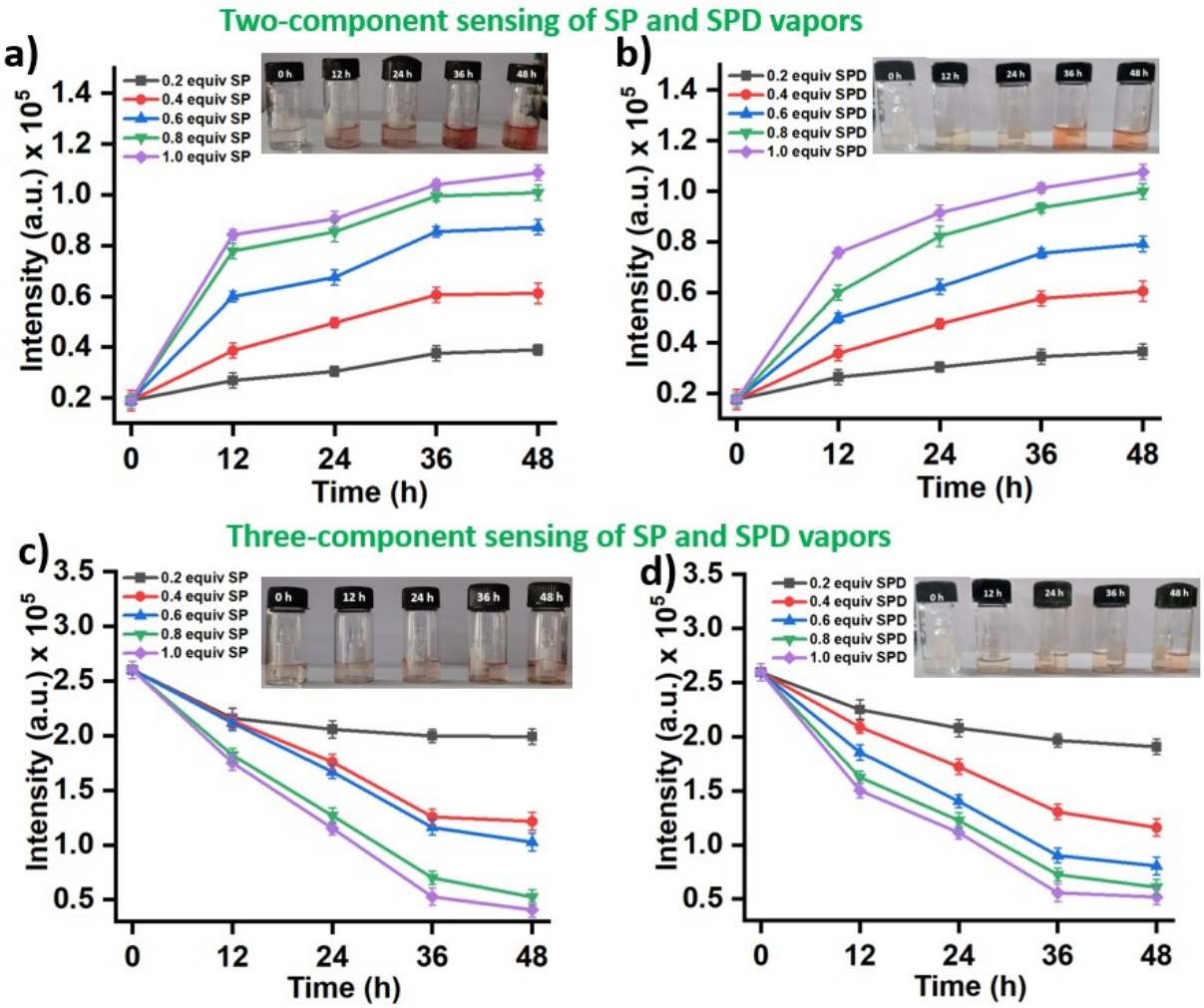

Figure S19. Time-dependent vapor phase sensing of spermine and spermidine at variable concentrations: The fluorescence responses from the two-component sensing assembly towards (a) spermine and (b) spermidine (**BPBP** (30 μM) + CB[7] (60 μM), λ_{ex} 519 nm, λ_{em} 730 nm); The fluorescence responses from three-component sensing assembly towards (c) spermine and (d) spermidine (GQDs (5 μL, 1 mg/mL) + **BPBP** (30 μM) + CB[7] (60 μM, λ_{ex} 370 nm, λ_{em} 535 nm); Insets: Corresponding visual color change images for the two-component and three-component sensors towards SP/SPD vapors after addition of 1 equiv of SP and 2 equiv of SPD, respectively.

Table S6. Vapor phase SP/SPD recovery data for the two-component and three-component supramolecular sensor[a]

Sr. No.	Sample	Spermine/ Spermidine added (μM)	Spermine/ Spermidine found (μM)	Recovery (%)	RSD (%) (n = 3)
1.	Two-component assembly (**BPBP** + CB[7]) + SP	06.0	05.011	83.5	2.7
		12.0	10.272	85.6	2.9
		18.0	15.102	83.9	3.4
		24.0	21.058	87.4	3.2
		30.0	25.530	85.1	3.0
2.	Two-component assembly (**BPBP** + CB[7]) + SPD	12.0	09.624	80.2	3.6
		24.0	19.560	81.5	2.9
		36.0	29.016	80.6	3.5
		48.0	40.080	83.5	2.4
		60.0	49.560	82.6	3.1
3.	Three-component assembly (GQDs + **BPBP** + CB[7]) + SP	06.0	05.412	90.2	2.8
		12.0	10.932	91.1	2.5
		18.0	16.128	89.6	3.3
		24.0	22.176	92.4	3.5
		30.0	27.450	91.5	3.1
4.	Three-component assembly (GQDs + **BPBP** + CB[7]) + SPD	12.0	10.788	89.9	2.8
		24.0	20.520	85.5	2.7
		36.0	31.536	87.6	3.6
		48.0	42.672	88.9	2.8
		60.0	53.760	89.6	2.4

[a]The maximum fluorescence intensities from the sensing solutions at 730 nm for two-component and at 535 nm for three-component supramolecular sensors, respectively after 48 h were plotted on the standard curves to obtain the % recovery data.

Table S7. A comparative study for dye-cavitand host-guest sensors of spermine/spermidine.

Sr. No.	Probe/dye Type	Strategy (host)	Detection Medium	Detection Limit	Analyte (BPAs)	Interference by other BPAs	Application	Ref. No
1.	Quinoline	host-guest (β-CD)	Glass Surface	Not Mentioned	SPD	NO	serum	2
2.	DASPI and Hoechst 33258	host-guest (CB[*n*], *n* = 6, 7, 8)	Tris-HCl buffer, pH 7.3	Not Mentioned	BPAs	Yes	NA	3
3.	PDI	host-guest (CB[7])	Highly acidic	30 nM	SP	SPD	NA	4
4.	TPE	host-guest (CB[7])	DMSO-H_2O	1.0 μM	SP	SPD, PUT	NA	5
5.	Phenazopyridine	host-guest (CB[7]) (Colorimetric)	Water	21 nM	SP	NO	Urine	6

6.	Gold nanoparticles	Pillar [5]arene (Colorimetric)	Water	0.034 μM	SP	NO	NA	7
7.	BPBP	host-guest (CB[7])	Water	20.2 ppb (SP), 36.3 ppb (SPD)	SP, SPD	NO	blood serum, urine	This work

BPAs: Biogenic polyamines; SP: Spermine; SPD: Spermidine; PDI: Perylene diimide; TPE: Tetraphenylethylene. [a]Unless otherwise mentioned the LOD presented in the table is for spermine.

Table S8. A comparative study for selected supramolecular sensing strategies for SP/SPD.

Sr. No.	Probe/dye Type	Detection Medium	Detection Limit (ppb)	Analyte (BPAs)	Ref. No.
1.	Functionalized MCM-41 loaded with Rhodamine 6G	Water	5463.2 (SP) 6545.2 (SPD)	SP and SPD	8
2.	Ciprofloxacin-Tb^{3+} complex	Water	34.3	SP	9
3.	Doxorubicin-ZnO-cucurbit[7]uril nanocomplex,	Water	Not mentioned	SP	10
4.	Quantum dots based nanoprobe	Water	40.5 (SP) 305 (SPD)	SP and SPD	11
5.	Pyrocatechol violet	HEPES buffer pH 7	1262	SP	12
6.	TPE	Phosphate buffer pH 7.4	141.7 (SP) 170.2 (SPD)	SP and SPD	13
7.	PDI-SDS	HEPES-buffered CH_3CN/H_2O (1:1, v/v, pH 7.2);	6.05	SP	14
8.	Squarine and Pyrene (micelles)	Water	957	SP	15

9.	Benzothiadiazole polymer-SDS	Water	66.8	SP	16
10.	Pyrene amphiphile	(0.8 mM MOPS, pH 7.0)	Not mentioned	SP	17
11.	CdTe QDs and carbon dots.	phosphate buffer (pH 8.0, 10 mM)	41 (SP) 305 (SPD)	SP and SPD	18
12.	TPE + CB[6]OH + HAp NPs	Water	1.4	SP, SPD	19
13.	**BPBP + GQD +CB[7] affinity-driven guest exchange**	**Water**	**0.1 (SP)** **0.9 (SPD)**	**SP, SPD**	**This work**

SP: Spermine; SPD: Spermidine; PDI: Perylenediimide; TPE: Tetraphenylethylene. [a]Unless otherwise mentioned the LOD presented in the table is for spermine

References:

1. L. Wang, Y. Wang, T. Xu, H. Liao, C. Yao, Y. Liu, Z. Li, Z. Chen, D. Pan, L. Sun and M. Wu, Gram-scale synthesis of single-crystalline graphene quantum dots with superior optical properties, *Nat Commun*. 2014, **5**, 5357, https://doi.org/10.1038/ncomms6357.
2. Y. Cheng, P. Jiang and X. Dong, Molecularly imprinted fluorescent chemosensor synthesized using quinoline-modified-β-cyclodextrin as monomer for spermidine recognition, *RSC Adv*. 2015, **5**, 55066−55074, https://doi.org/10.1039/C5RA07761C.
3. K. M. Park, J. Kim, Y. H. Ko, Y. Ahn, J. Murray, M. Li, A. Shrinidhi and K. Kim, Dye-cucurbit[n]uril complexes as sensor elements for reliable pattern recognition of biogenic polyamines, *Bull. Chem. Soc. Jpn*. 2018, **91**, 95−99, https://doi.org/10.1246/bcsj.20170302.
4. K. Liu, Y. Yao, Y. Kang, Y. Liu, Y. Han, Y. Wang, Z. Li and X. Zhang, A supramolecular approach to fabricate highly emissive smart materials, *Sci. Rep*. 2013, **3**, 2372−2379, https://doi.org/10.1038/srep02372.
5. G. Jiang, W. Zhu, Q. Chen, X. Li, G. Zhang, Y. Li, X. Fan and J. Wang, Selective fluorescent probes for spermine and 1-adamantanamine based on the supramolecular structure formed between AIE-active molecule and cucurbit[n]urils, *Sens. Actuators, B* 2018, **261**, 602−607, https://doi.org/10.1016/j.snb.2018.01.197.
6. H. Zhang, M. Liu, X. Zhu and H. Li, Detection of spermine using cucurbit[7]uril-phenazopyridine host-guest inclusion complex as a platform, *Chem. Lett*. 2021, **50**, 154–157, https://doi.org/10.1246/cl.200667.
7. X. Tan, X. Liu, W. Zeng, Z. Zhang, T. Huang, L. Yu and G. Zhao, Colorimetric sensing towards spermine based on supramolecular pillar[5]arene reduced and stabilized gold nanoparticles, *Spectrochim. Acta, Part A* 2019, **221**, 117176, https://doi.org/10.1016/j.saa.2019.117176.

8. M. Barros, A. López-Carrasco, P. Amorós, S. Gil, P. Gaviña, M. Parra, J. E. Haskouri, M. C. Terencio and A. M. Costero, Chromogenic chemodosimeter based on capped silica particles to detect spermine and spermidine, *Nanomaterials* 2021, **11**, 818, https://doi.org/10.3390/nano11030818.
9. N. N. Nghia, B. T. Huy, P. T. Phong, J. S. Han, D. H. Kwon and Y. -I. Lee, Simple fluorescence optosensing probe for spermine based on ciprofloxacin-Tb^{3+} complexation, *PLoS ONE* 2021, **16**, e0251306, https://doi.org/10.1371/ journal.pone.0251306.
10. Y. Chen, L. Jing, Q. Meng, B. Li, R. Chen and Z. Sun, Supramolecular chemotherapy: Noncovalent bond synergy of cucurbit[7]uril against human colorectal tumor cells, *Langmuir* 2021, **37**, 9547−9552, https://doi.org/10.1021/acs.langmuir.1c01422.
11. S. Abbasi-Moayed, A. Bigdeli and M. R. Hormozi-Nezhad, Determination of spermine and spermidine in meat with ratiometric fluorescence nanoprobe and a combinational logic gate, *Food Chem*. 2022, **384**, 132459, http:/doi.org/10.1016/j.foodchem.2022.132459.
12. Y. Fukushima, and S. Aikawa, Colorimetric chemosensor for spermine based on pyrocatechol violet and anionic phenylboronic acid in aqueous solution, *Microchem. J.* 2021, **162**, 105867, http:/doi.org/10.1016/j.microc.2020.105867.
13. M. Barros, S. Ceballos, P. Arroyo, J. A. Sáez, M. Parra, S. Gil, A. M. Costero and P. Gaviña, Spermine and spermidine detection through restricted intramolecular rotations in a tetraphenylethylene derivative, *Chemosensors* 2022, **10**, 8, https://doi.org/10.3390/chemosensors10010008.
14. P. Singh, L. S. Mittal, G. Bhargava and S. Kumar, Ionic self-assembled platform of perylenediimide–sodium dodecylsulfate for detection of spermine in clinical samples, *Chem. Asian J*. 2017, **12**, 890–899, https://doi.org/10.1002/asia.201700120.

15. J. Tu, S. Sun and Y. Xu, A novel self-assembled platform for the ratiometric fluorescence detection of spermine, *Chem. Commun*. 2016, **52**, 1040–1043, https://doi.org/10.1039/c5cc07861j.

16. A. H. Malik, S. Hussain and P. K. Iyer, Aggregation-induced FRET via polymer−surfactant complexation: A new strategy for the detection of spermine, *Anal. Chem*. 2016, **88**, 7358−7364, https://doi.org/10.1021/acs.analchem.6b01788.

17. Z. Köstereli and K. Severin, Fluorescence sensing of spermine with a frustrated amphiphile, *Chem. Commun.* 2012, **48**, 5841–584310, https://doi.org/1039/c2cc32228e.

18. V. G. Naik, V. Kumar, A. C. Bhasikuttan, K. Kadu, S. R. Ramanan, A. A. Bhosle, M. Banerjee and A. Chatterjee, Solid-supported amplification of aggregation emission: A tetraphenylethylene−cucurbit[6]uril@hydroxyapatite-based supramolecular sensing assembly for the detection of spermine and spermidine in human urine and blood, *ACS Appl. Bio Mater*. 2021, **4**, 1813–1822, https://doi.org/10.1021/acsabm.0c01527.

NMR Spectra:

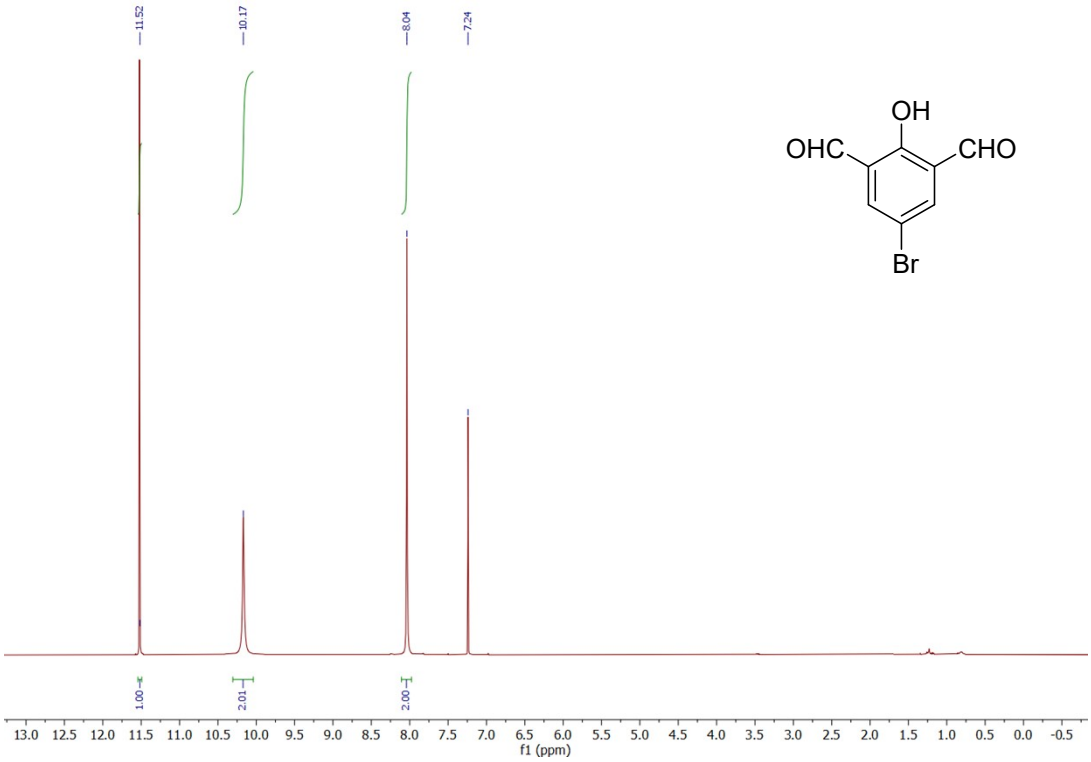

^{1}H NMR spectrum of **5-bromo-2-hydroxyisophthalaldehyde**.

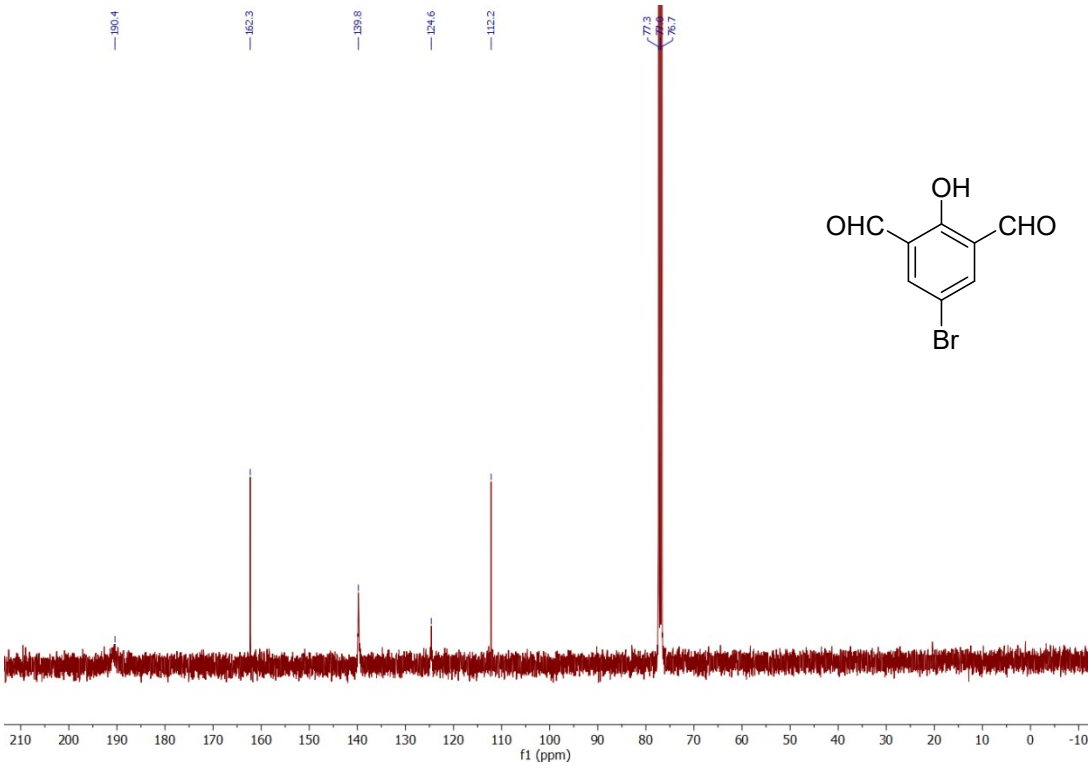

^{13}C NMR spectrum of **5-bromo-2-hydroxyisophthalaldehyde**.

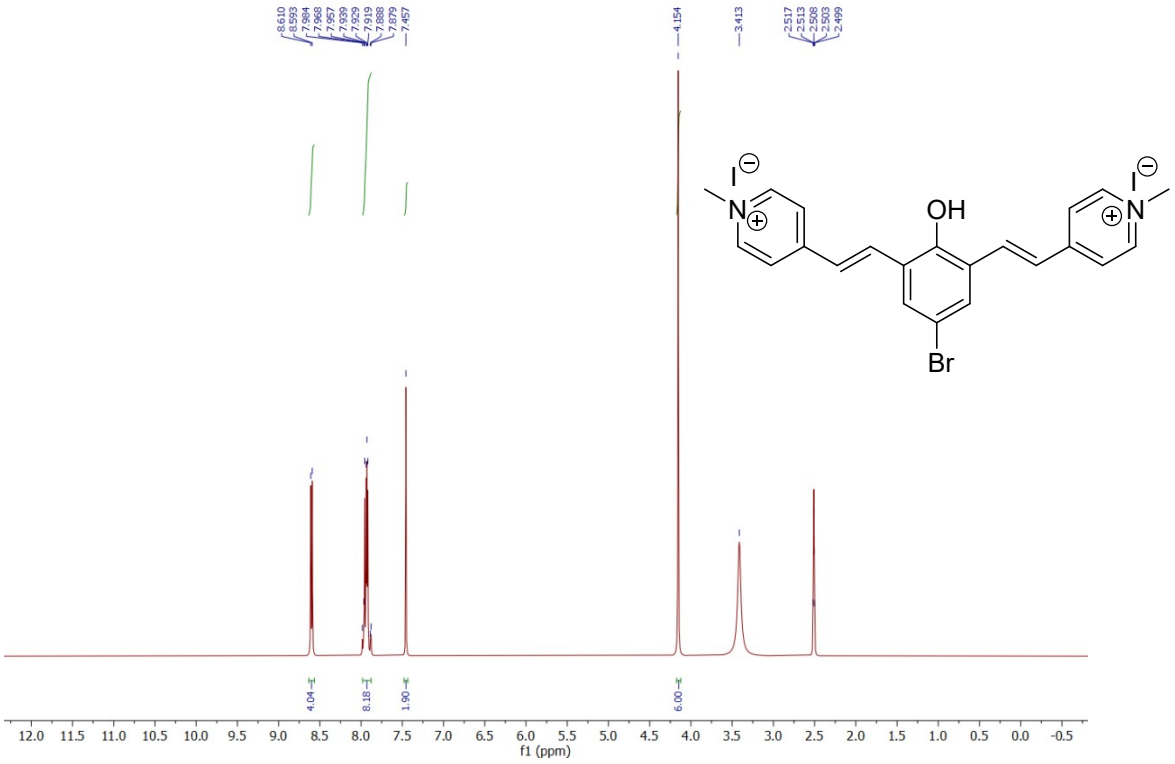

^{1}H NMR spectrum of **BPBP**.

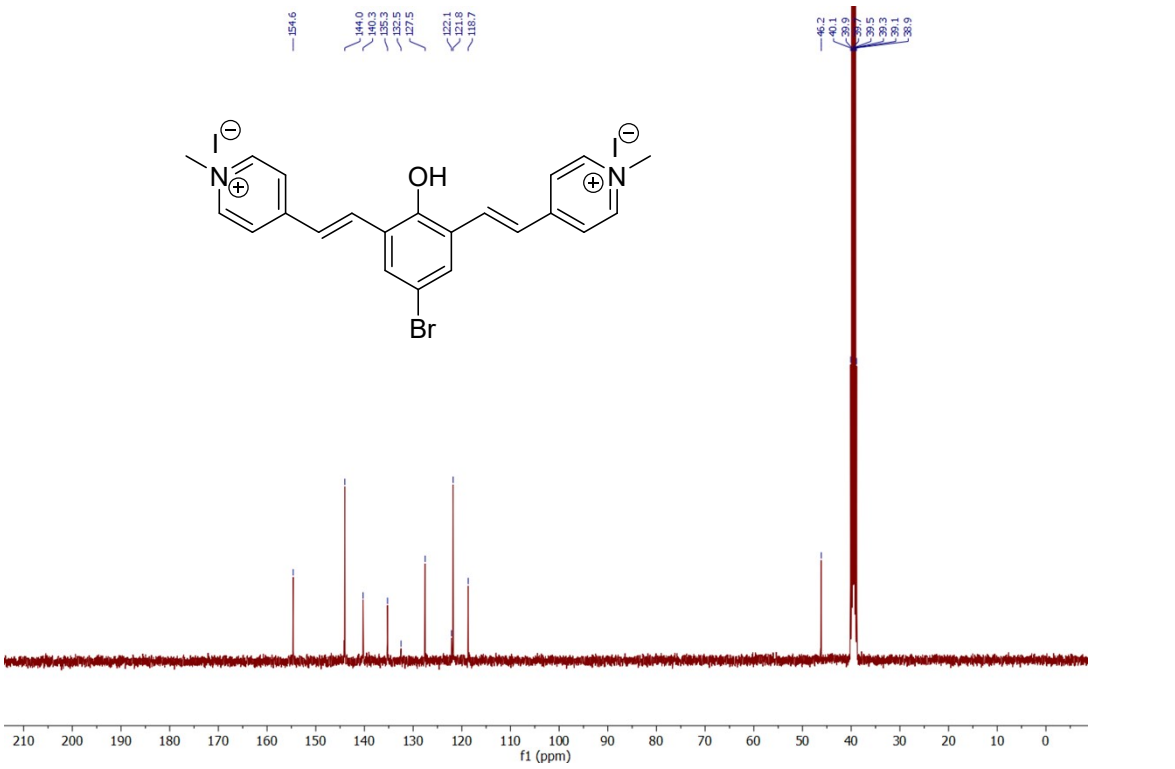

^{13}C NMR spectrum of **BPBP**.